

**MAXIMUM TOLERATED ACTIVITY
ESTIMATION BASED ON RED MARROW DOSE
USING MULTIPLE DOSIMETRY APPROACHES
IN RADIOIODINE THERAPY SURROGATED BY
IODINE-124**

NG YI HAN

**SCHOOL OF HEALTH SCIENCES
UNIVERSITI SAINS MALAYSIA**

2024

**MAXIMUM TOLERATED ACTIVITY
ESTIMATION BASED ON RED MARROW DOSE
USING MULTIPLE DOSIMETRY APPROACHES
IN RADIOIODINE THERAPY SURROGATED BY
IODINE-124**

by

NG YI HAN

**Dissertation submitted in partial fulfilment of the requirements for the degree of
Bachelor of Health Science (Honours) (Medical Radiation)**

July 2024

DECLARATION

I hereby declare that this dissertation is the results of my own investigations, except where otherwise stated and duly acknowledged. I also declare that it has not been previously or concurrently submitted as a whole for any other degrees at Universiti Sains Malaysia or other institutions. I grant Universiti Sains Malaysia the right to use the dissertation for teaching, research and promotional purpose.



NG YI HAN

Date: 23-06-2024

ACKNOWLEDGEMENT

This thesis would not have been possible without the guidance and the help of several individual who in one way or another contributed and extended their valuable assistance in the preparation and completion of this study, it is a pleasure to thank those who made it a possibility.

First and foremost, I am extremely grateful to my main supervisor, Dr. Marianie binti Musarudin, for her unwavering support and insightful guidance throughout my bachelor's study. Her expertise and dedication were invaluable in shaping my research and helping me navigate the complexities of my project. I also extend my sincere thanks to my co-supervisors Dr. Mohamad Aminudin Bin Said physicist of the Nuclear Medicine Department at Institute Kanser Negara for inviting me to work on my research project in collaboration with Institut kanser Negara and Dr. Mohammad Khairul Azhar Abdul Razab chairperson of Medical Radiation Programme at Universiti Sains Malaysia for his continuous support in sharing his expertise and knowledge in nuclear medicine to improve my research project. Their immense knowledge and plentiful experience have encouraged me in all the time of my academic research and daily life. I would also like to thank Puan Umami Habibah binti Ibarhim medical physicist at the Nuclear Medicine Department of Institut Kanser Negara for her technical support and assistance in data collection on my study. Her help was indispensable and greatly appreciated.

I am deeply thankful to my parents, family members, and friends for their kind support and encouragement throughout this research project. Lastly, I would like to acknowledge those who directly or indirectly lent their hand to this venture.

TABLE OF CONTENTS

CERTIFICATE.....	ii
DECLARATION.....	iv
ACKNOWLEDGEMENT	v
TABLE OF CONTENTS	vi
LIST OF TABLES.....	x
LIST OF FIGURES.....	xi
LIST OF SYMBOLS	xiv
LIST OF ABBREVIATIONS.....	xvii
LIST OF APPENDICES	xix
ABSTRAK	xx
ABSTRACT.....	xxii
CHAPTER 1	1
INTRODUCTION	1
1.1 Background of the Study.....	1
1.2 Problem Statement	5
1.3 Study Objectives	7
1.3.1 General Objectives	7
1.3.2 Specific Objectives.....	7
1.4 Study Hypothesis	7
1.4.1 Null Hypothesis.....	7
1.4.2 Alternative Hypothesis	8
1.5 Significance of the Study	8
1.6 Conceptual Framework	9
CHAPTER 2	10
LITERATURE REVIEW	10

2.1 Radioiodine Therapy	10
2.1.1 The European Association of Nuclear Medicine Blood-based dosimetry practiced by IKN.	11
2.1.2 Red Marrow as an Organ at Risk	15
2.1.3 The Rationale of Absorbed Dose of Blood, Red Marrow and Blood Dose per Activity.....	16
2.2 Multiple Dosimetry Approaches	18
2.2.1 Image-based dosimetry	18
2.2.2 Simplified Image-based dosimetry	21
2.2.3 Red Marrow-based (OLINDA).....	23
CHAPTER 3	25
METHODOLOGY.....	25
3.1 Study Design	25
3.2 Study Flowchart	26
3.3 Study Location	27
3.4 Target Population	27
3.5 Selection Criteria.....	27
3.5.1 Inclusion Criteria.....	27
3.5.2 Exclusion Criteria.....	27
3.6 Sample Size.....	27
3.7 Sampling Method	28
3.8 Study Instruments	28
3.9 Data Collection.....	29
3.10 Methodology	29
3.10.1 Image-based dosimetry	30
3.10.2 RM-based dosimetry	31
3.10.3 Simplified image-based dosimetry.....	32
3.11 Data Analysis.....	33

3.12 Ethical Clearance	34
CHAPTER 4	35
RESULTS.....	35
4.1 Estimation of Blood (τ_{BL}), Red-Marrow (τ_{RM}), and Whole-body Residence Time (τ_{WB}).....	35
4.2 Calculation of BDpA Based on The Investigated Dosimetry Approaches.	36
4.3 Determination of the Personalized MTA of ^{131}I Based on the BDpA Derived from the Investigated Dosimetry Approaches.....	37
4.4 Correlation Between EANM Blood-Based Dosimetry Approach and Different Dosimetry Approaches	38
4.5 Statistical Analysis for the Significant Differences Between MTA Estimated by EANM Blood-Based Approach and Different Dosimetry Approaches	40
CHAPTER 5	42
DICUSSION	42
5.1 Significant Differences Between MTA Estimated by EANM Blood-Based Approach and Three Other Studied Dosimetry Approaches.	46
5.2 Correlation Between EANM blood-based dosimetry approach and three other dosimetry approaches.....	47
5.3 Limitation of the Study	47
CHAPTER 6	49
CONCLUSION.....	49
6.1 Overall Findings of This Study	49
6.2 Recommendation for Future Research.....	49
REFERENCES.....	51
APPENDICES	57
APPENDIX A	57
APPENDIX B	58
APPENDIX C	60

APPENDIX D	64
APPENDIX E	66
APPENDIX F.....	69
APPENDIX G	73

LIST OF TABLES

Table 1.1 Types of dosimetry approaches investigated in this study.....	2
Table 4.1(a) The derived Blood (τ_{BL}) and Red-Marrow (τ_{RM}) residence time.....	35
Table 4.1(b) The derived whole-body residence time (τ_{WB}).....	36
Table 4.2 The BDpA calculated using multiple dosimetry approaches.	37
Table 4.3 Personalized MTA calculation based on the BDpA calculated using multiple dosimetry approaches.....	38
Table 4.4 Correlation between the BDpA derived from EANM blood-based dosimetry approach and three other dosimetry approaches.	39
Table 4.5 Significant difference between the MTA estimated by EANM blood-based dosimetry approach and three other dosimetry approaches. (n=24)	41
Table B.1 Study participants' demographic and pre-therapeutic EANM blood-based dosimetry assessment data	58
Table B.2 Study participant's volume and integral activity data of vertebrae (L2-L4) and whole body.	59

LIST OF FIGURES

Figure 1.1 Conceptual framework.....	9
Figure 2.1 Flowchart of Pre-Therapeutic Blood Based Dosimetry Assessment Practiced By IKN.	15
Figure 3.1 Study flowchart.....	26
Figure 3.2 Contoured Lumbar Vertebrae L2 – L4 and whole-body in subject’s CT image.....	31
Figure 3.2 Study flowchart.....	35
Figure 3.1 A scatter plot showing a not significant and weak positive correlation between the BDpA calculated using EANM blood-based and image-based dosimetry approaches.....	39
Figure 4.2 A scatter plot showing a not significant and strong positive correlation between the BDpA calculated using EANM blood-based and RM-based dosimetry approaches.....	39
Figure 4.3 A scatter plot showing a not significant and weak positive correlation between the BDpA calculated using EANM blood-based and simplified image-based dosimetry approaches.....	40
Figure C.1 Radionuclide input in OLINDA/EXM Software Version 1.1	60
Figure C.2 Phantom model selection in the OLINDA/EXM Software Version 1.1 ..	60
Figure C.3 Determination of the RM residence time based on the ¹³¹ I RM uptake value using tri-exponential curve.....	61
Figure C.4 Determination of the WB residence time based on the ¹³¹ I RM uptake value using bi-exponential curve.	61

Figure C.5 Input of the RM and whole-body residence time into the OLINDA/EXM Software Version 1.1	62
Figure C.6 Modification of input data based on the patient's RM mass and total body mass.....	62
Figure C.7 DRM computed by the OLINDA/EXM Software Version 1.1.....	63
Figure D.1 Spread sheet selection and demographic data input for the simplified Excel spread sheet.....	64
Figure D.2 Time point and whole-body integral activity input.....	64
Figure D.3 Mono-exponential curve generated and yielded τ_{WB} and τ_{RM}	65
Figure D.4 BDpA and MTA computed based on linear S-factor scaling method.....	65
Figure E.1 PET/CT images import from IKN database.....	66
Figure E.2 Contouring done at the lumbar vertebrae L2 in patient's CT image.....	66
Figure E.3 Contouring done for WB in patient's CT image.....	67
Figure E.4 Image fusion between CT image and PET images at three time points...	67
Figure E.5(a) Result for image analysis at contoured lumbar vertebrae L2 to L4.....	68
Figure E.5(b) Result for image analysis at contoured whole-body.....	68
Figure F.1 Asymmetrical distribution of the BDpA calculated based on the EANM blood-based dosimetry approach.....	69
Figure F.2 Asymmetrical distribution of the BDpA calculated based on the Image-based dosimetry approach.....	69
Figure F.3 Asymmetrical distribution of the BDpA calculated based on the RM-based dosimetry approach.....	70
Figure F.4 Asymmetrical distribution of the BDpA calculated based on the simplified image-based dosimetry approach.....	70

Figure F.5 Asymmetrical distribution of the MTA calculated based on the EANM blood-based dosimetry approach.....	71
Figure F.6 Asymmetrical distribution of the MTA calculated based on the Image- based dosimetry approach.....	71
Figure F.7 Asymmetrical distribution of the MTA calculated based on the RM-based dosimetry approach.....	72
Figure F.8 Symmetrical distribution of the MTA calculated based on the simplified image-based dosimetry approach.....	72

LIST OF SYMBOLS

e	Mathematical constant
t	Time/time point
λ	Fit constant
W	Patient's weight
H	Patient's height
Bqml	Integral Activity
GBq	Giga-becquerel
Gy	Gray
keV	Kilo electron volt
h	Hour(s)
mCi	Milli-Curie
ml	Milliliter
^{124}I	Iodine-124
^{131}I	Iodine-131
$A(t)$	Activity at time point
A_0	Administered tracer activity
\tilde{A}	Cumulated Activity
\widetilde{A}_{ROB}	Cumulated Activity of rest of the body
\widetilde{A}_{BL}	Cumulated Activity of blood
D	Absorbed dose
\bar{D}	Mean absorb dose
D_{BL}	Blood absorbed dose

D_{RM}	Red marrow absorbed dose
$\tilde{D}_{RM \leftarrow RM}$	Mean absorbed dose of red marrow contributed by red marrow
$\tilde{D}_{RM \leftarrow WB}$	Mean absorbed dose of red marrow contributed by whole body
NaI-124	Sodium 124-iodide
$U_{124}(t)$	Measured ^{124}I -based uptake values
$U_{131}(t)$	Projected ^{131}I -based uptake values
$T_{p124}(t)$	Physical half-life of ^{124}I
$T_{p131}(t)$	Physical half-life of ^{131}I
S_a	Surface area
S	Mean absorbed dose in target organ per decay in source organ
S_{RM}	Red Marrow S-value
S_{BL}	Blood S-value
S_{WB}	Whole-body S-value
$S_{RM \leftarrow RoB, patient}$	Mean absorbed dose by red marrow delivered per unit activity preset in the rest of the body of patient
$S_{RM \leftarrow RoB, phantom}$	Mean absorbed dose by red marrow delivered per unit activity preset in the rest of the body of phantom
τ	Residence time
$\tau_{BL}^{1 ml}$	Residence time in 1 ml of blood
τ_{BL}	Blood Residence time
τ_{RM}	Red Marrow Residence time
τ_{WB}	Whole-body residence time
τ_{RoB}	Remaining of body residence time
m_{WB}	Patient's whole-body mass

$m_{WB,patient}$	Patient's whole-body mass
$m_{WB,phantom}$	Phantom's whole-body mass
$m_{RM,patient}$	Patient's red marrow mass
$m_{RM,phantom}$	Phantom's red marrow mass
$m_{L2-L4}^{patient}$	Patient's lumbar vertebrae L2 to L4 trabecular bone marrow mass
m_{L2-L4}^{refman}	Reference lumbar vertebrae L2 to L4 trabecular bone marrow mass
$V_{trab L2-L4}^{patient}$	Patient's lumbar vertebrae L2 to L4 trabecular bone volume
$V_{trab L2-L4}^{refman}$	Reference man lumbar vertebrae L2 to L4 trabecular bone volume

LIST OF ABBREVIATIONS

RAI	Radioactive Iodine
BDpA	Blood Dose per Activity
CT	Computed tomography
DTC	Differentiated thyroid cancer.
EANM	European Association of Nuclear Medicine
FAA	Fraction of the administered activity
IKN	Institut Kanser Negara
IQR	Interquartile range
MC	Monte-Carlo
MIRD	Medical International Radiation Dose
MREC	Medical Research and Ethics Committee
MTA	Maximum tolerated activity
NIH	National Institutes of Health
PET	Positron Emission Tomography
OAR	Organ at risk
OLINDA/EXM	Organ Level Internal Dose Assessment/Exponential Modelling
RADAR	Radiation Dose Assessment Resource
RM	Red marrow
RMBLR	Red marrow to blood ratio
RMECFE	Red marrow extra cellular fluid fraction
RoB	Remaining of body
SD	Standard Deviation

SPSS	Statistical package for Social Sciences
TBV	Total blood volume
WB	Whole body
PET/CT	Positron emission tomography/ Computed tomography

LIST OF APPENDICES

APPENDIX A	Data collection form
APPENDIX B	Data retrieved from IKN's database
APPENDIX C	Flow chart of the OLINDA/EXM software
APPENDIX D	Flow chart of the simplified image-based dosimetry approach using a simplified Excel spreadsheet for BDpA computation
APPENDIX E	Flow chart for PET/CT image analysis using MIM software version 7.3.5
APPENDIX F	Normality test results
APPENDIX G	Ethical approval letter from MREC under MOH

**ANGGARAN AKTIVITI TERTOLERAN MAKSIMUM
BERDASARKAN DOS SUMSUM TULANG MERAH
MENGUNAKAN PENDEKATAN DOSIMETRI PELBAGAI
DALAM TERAPI RADIOIODIN YANG DIGANTIKAN OLEH
IODIN-124**

ABSTRAK

Penilaian dosimetri berdasarkan darah pra-terapeutik berfungsi sebagai alternatif kepada protokol dos empirikal terapi radioiodin (^{131}I) untuk merawat pesakit kanser tiroid terbeza (DTC) dengan keadaan tidak normal. Ia bertujuan untuk menyesuaikan aktiviti maksimum toleransi (MTA) ^{131}I yang lebih berkesan secara individu dengan menganggarkan dan memastikan bahawa dos terserap yang dihasilkan di dalam darah atau sumsum tulang merah (D_{BL} atau D_{RM}) kekal dalam lingkungan 2 Gy untuk mencegah ketoksikan mieloma. Sehingga kini, Institut Kanser Negara (IKN) bergantung sepenuhnya kepada kaedah dosimetri EANM berdasarkan darah untuk menganggarkan D_{BL} . Kajian ini bertujuan untuk membandingkan kaedah ini dengan tiga kaedah lain yang belum pernah dikaji sebelum ini dari segi korelasi dan perbezaan yang ketara. **Perancangan:** Data demografi, dosimetri dan gambar PET/CT bagi 12 pesakit DTC dewasa yang menjalani penilaian dosimetri berdasarkan darah pra-terapeutik ^{131}I diperolehi untuk pengiraan dos dalam kajian retrospektif ini. Kaedah dosimetri termasuk kaedah berdasarkan gambar, kaedah sumsum tulang merah dan kaedah berdasarkan gambar yang disederhanakan. **Keputusan:** Kedua-dua kaedah berdasarkan gambar ($r = 0.194$) dan kaedah berdasarkan gambar yang disederhanakan ($r = 0.194$) menunjukkan korelasi positif lemah manakala kaedah RM menunjukkan korelasi positif yang kuat ($r = 0.540$) apabila dibandingkan dengan dos darah bagi setiap hasil aktiviti oleh kaedah EANM berdasarkan darah. Walau bagaimanapun, tiada korelasi yang ketara secara statistik, seperti yang ditunjukkan oleh ujian korelasi

Spearman's rank ($p > 0.05$). Apabila menilai nilai MTA, kedua-dua kaedah berdasarkan gambar ($P = 0.015$) dan kaedah RM ($P = 0.013$) menunjukkan perbezaan yang ketara berbanding dengan kaedah EANM berdasarkan darah. Sebaliknya, kaedah berdasarkan gambar yang disederhanakan tidak menunjukkan perbezaan median MTA yang ketara berbanding dengan kaedah EANM berdasarkan darah, disokong oleh ujian Mann-Whitney ($p > 0.05$). **Kesimpulan:** IKN dicadangkan untuk mengamalkan kaedah berdasarkan gambar sebagai pematuhan piawai di bawah semua keadaan kerana penganggaran MTA individu adalah lebih sensitif dan memastikan keselamatan radiasi kepada para pesakit IKN.

MAXIMUM TOLERATED ACTIVITY ESTIMATION BASED ON RED MARROW DOSE USING MULTIPLE DOSIMETRY APPROACHES IN RADIOIODINE THERAPY SURROGATED BY IODINE-124

ABSTRACT

Pre-therapeutic blood-based dosimetry assessment serves as an alternative to the empirical dosage protocol of radioiodine (^{131}I) therapy for treating differentiated thyroid cancer (DTC) patients with a typical condition. It aims to customize a more effective personalized maximum tolerated activity (MTA) of ^{131}I by estimating and ensuring that the resulting absorbed dose in either the blood or red marrow (D_{BL} or D_{RM}) remains within 2 Gy to prevent myelotoxicity. Currently, the Institute Kanser Negara (IKN) relies exclusively on the EANM blood-based dosimetry approach for estimating D_{BL} . This study seeks to compare this approach with three other approaches that have not been previously explored in terms of their correlation and significant differences. **Methods:** The demographic, dosimetry data and PET/CT images of 12 adult DTC patients who underwent the pre-therapeutic blood-based dosimetry assessment of ^{131}I therapy were retrieved for the dose computation in this retrospective study. Dosimetry approaches include the image-based, red marrow-based and simplified image-based approaches. **Results:** Both image-based ($r = 0.194$) and simplified image-based approaches ($r = 0.194$) demonstrated weak positive correlations while RM-based approach displayed a strong positive correlation ($r = 0.540$) when compared to blood dose per activity yield by EANM blood-based approach. However, none of these correlations were statistically significant, as indicated by Spearman's rank correlation test ($p > 0.05$). When evaluating MTA values,

both the image-based and RM-based approaches displayed significant disparities compared to the EANM blood-based approach, with p-values of 0.015 and 0.013, respectively. Conversely, the simplified image-based approach demonstrated no statistically significant difference in estimated MTA compared to the EANM blood-based approach, supported by the Mann-Whitney test ($p > 0.05$). **Conclusion:** It is recommended for IKN to adopt the image-based approach as the standard formalism under all circumstances due to its sensitivity in estimating personalized MTA and ensuring radiation safety.

CHAPTER 1

INTRODUCTION

1.1 Background of the Study

Radioiodine (RAI) therapy using Iodine-131 (^{131}I) has been a long-standing approach for treating thyroid cancer (Erdi et al., 1999). Enhancing the effectiveness of therapy for metastases can be achieved by using higher doses of ^{131}I . When dealing with metastatic cancer, it is common to administer an empirical radioactive iodine activity ranging from 3.7 to 7.4 GBq ^{131}I (Luster et al., 2008; Jentzen et al., 2015). However, the amount of ^{131}I that can be administered is restricted due to the potential for severe radiation-related harm to vital organs. In many cases, the absorbed radiation dose in the red marrow is the primary limiting factor (Jentzen et al., 2015). The red marrow dose limit of 2 gray (Gy) was first established by Benua et al. during the early 1960s. While RAI therapy is typically a safe and effective treatment for thyroid cancer when administered at appropriate levels, it's crucial to acknowledge that doses surpassing 5.55 to 7.4 GBq (or 150 to 200 mCi) can frequently subject older patients' bone marrow to more than 2 Gy of radiation (Jentzen et al., 2015). In radiation therapy, the red marrow (RM) refers to the sensitive blood-forming cells within the bone marrow, and it is essential to protect these cells during ^{131}I therapy as it is considered the critical organ at risk (OAR) (Schwartz et al., 2012).

Dosimetry Approach
EANM Blood-based
Image-based
Red Marrow-based
Simplified Image-based

Table 1.1 Types of dosimetry approaches investigated in this study.

In the 1950s, dosimetry methods were developed to evaluate the retention of radioactive iodine in the body and to estimate the absorbed doses in the blood and bone marrow. These methods allow healthcare professionals to determine the maximum tolerated activity (MTA) of RAI which represents the maximum amount that can be safely administered without causing harmful effects on the bone marrow (Tuttle et al., 2006). Referring to the Table 1.1, there are several methods of dosimetry in the 21st century, which include the blood-based dosimetry, image-based dosimetry, and red marrow-based dosimetry. Blood-based dosimetry is a straightforward and invasive approach that assesses the RAI activity in the blood and uses it to estimate the absorbed dose in the RM (Wessels et al., 2004). Image-based dosimetry utilizes tomographic image data, such as computed tomography (CT) scans, to segment organs and calculate the absorbed dose rate per unit of activity. Advanced image-based dosimetry uses voxel-level dosimetry products such as fast Monte Carlo (MC) algorithm to simulate an activity distribution based on serial single-photon emission computed tomography (SPECT) or positron emission tomography (PET) images, along with CT scans, to generate a dose map. This method is typically employed for customized RAI therapy (Beauregard, 2022). Red marrow-based dosimetry is a subset of organ-based dosimetry that concentrates on determining the absorbed dose in specific organs or

tissues, particularly the red marrow in our study (Capala et al., 2021). Products like the Organ Level Internal Dose Assessment/Exponential Modelling (OLINDA/EXM) software (version 1.1) which utilizes a kinetic model and established human body models found in existing scientific literature to calculate estimates of the radiation dose to all organs and the entire body (Jeffrey A. Siegel et al., 2023). In short, for all the dosimetry models explained the ultimate aim is to estimate the MTA for ^{131}I therapy.

Since 2015 Nuclear Medicine Department in Institut Kanser Negara (IKN) had adapt personalise ^{131}I therapy for patient that failed to recover from empirical treatment by performing pre-therapeutic dosimetry for each patient. In this study, Iodine-124 Positron Emission Tomography/Computed Tomography (PET/CT) scanning was used to surrogate ^{131}I for dosimetry purposes. ^{124}I , a PET/CT radiotracer with a half-life of 4.2 days, provides enhanced imaging capabilities, including improved spatial resolution and sensitivity achieved through coincidence detection on PET/CT scanners. Additionally, its relatively long half-life allows for the assessment of iodine kinetics within the body (Kuker et al., 2017). Subsequent research has highlighted the clinical significance of I-124 PET/CT for detecting residual thyroid tissue and metastasis in differentiated thyroid cancer (DTC) patients (Mya Thaug, 1956). The first PET-based dosimetry study in DTC patients was published in 1999, demonstrating the feasibility of quantification after phantom studies. . PET/CT and SPECT are imaging techniques offering 3D quantitative insights into human physiology. PET/CT stands out with better attenuation correction for precise radiation dose estimation in terms of absolute activity concentration in patient body for example Becquerel per volume (Bq/ml) and enhanced sensitivity and spatial resolution compared to SPECT and planar γ -camera imaging which is vital for accurate tissue and organ dose assessment (Kuker et al., 2017).

The focus of this study is the pre-therapeutic MTA estimation using image-based and RM-based dosimetry approach. Quantitative imaging accounts the variations in individual marrow mass, the calculation involved estimating RM mass of the patient from the lumbar vertebrae (L2-L4) by scaling it with the Reference Man's trabecular bone volume. While RM-based method will use total blood volume (TBV) as surrogate to RM mass. The aim of this study is to compare the results of the estimation of blood dose per activity (BDpA) and MTA using different approaches. This study will be beneficial for both patient and personnel in IKN as it allows the determination of a better and safe approach in estimating MTA, while reduce the burden of patient and personnel for drawing blood at each time points.

1.2 Problem Statement

Starting in 2015, IKN has exclusively utilised the European Association of Nuclear Medicine (EANM) blood-based dosimetry to estimate the MTA from absorbed dose to blood (D_{BL}) as a surrogate for absorbed dose to red marrow (D_{RM}) in the pre-therapeutic blood-based dosimetry assessment. This approach is employed to calculate the individualized MTA of ^{131}I for patients with DTC, especially those who have not responded or are unsuitable for the empirical dose approach. Despite the blood-based dosimetry, there exist several well-established dosimetry approaches that could potentially provide accurate MTA estimation, but these have not been practiced by IKN. For example, image-based dosimetry (Ferrer et al., 2010), RM-based dosimetry (Jeffrey A. Siegel et al., 2023), and simplified image-based dosimetry (Songprakhon et al., 2020) are among the alternatives. To date, a universally accepted and widely adopted dosimetry approach for MTA estimation is not well documented. Consequently, variations in the estimated MTA have been noted across different institutions, as they may opt to implement various dosimetry approach. (Hindorf et al., 2010; Pandit-Taskar et al., 2021; Schwartz et al., 2012).

The EANM Dosimetry Committee Series guidelines recommend the practical adoption of the EANM blood-based dosimetry model, primarily with a focus on radiation safety. This is because the model yields lower MTA estimates due to its higher estimated D_{BL} (Hindorf et al., 2010). However, it's important to note that the EANM blood-based dosimetry model cannot account for the specific uptake of any radiopharmaceutical in the bone marrow compartment (Ferrer et al., 2010). Moreover, when estimating red marrow self-dose, blood-based dosimetry can result in substantial discrepancies, ranging from -74% to 62% in individual patients, particularly in the context of ^{124}I -labeled antibodies, as opposed to PET/CT image-based dosimetry

(Lassmann et al., 2008). Additionally, blood-based dosimetry is an invasive procedure which might cause extravasation that can be burdensome for patients as it necessitates blood sampling for measuring blood radioactivity.

^{124}I which is commonly used as a surrogate to ^{131}I in pre-therapeutic dosimetry, offers a higher-resolution PET/CT images, thus enabling more precise dosimetry calculations (Kuker et al., 2017). The superiority of ^{124}I PET/CT imaging in image-based dosimetry for red marrow dosimetry in comparison to blood-based methods was previously emphasized (Schwartz et al., 2012). In line with that, a retrospective study on ^{124}I PET/CT dosimetry revealed a good correlation between higher lesion absorbed dose (AD), biological effective dose (BED), and equivalent uniform dose (EUD), which indicating a better response to ^{131}I therapy (Plyku et al., 2022). Based on the argument, it is valuable to investigate a non-invasive dosimetry approach, particularly the image-based and simplified image-based approaches to estimate the MTA to be prescribed to the patient. This study is therefore aimed to compare the EANM blood-based dosimetry approach practiced by IKN and other three different dosimetry approaches (RM-based, image-based and simplified image-based) in terms of their correlation in blood dose per activity (BDpA) calculation and significant differences in MTA estimation to suggest a reliable standard approach in future pre-therapeutic dosimetry assessment.

1.3 Study Objectives

1.3.1 General Objectives

The general objective of this study is to conduct a comparative analysis of blood dose per activity (BDpA) and maximum tolerated activity (MTA) through EANM blood-based dosimetry practiced by IKN, contrasting it with image-based and RM-based approaches, to assess pre-therapeutic dosimetry for ^{131}I therapy in patients with differentiated thyroid cancer (DTC).

1.3.2 Specific Objectives

1. To determine the significant difference between the MTA calculated by EANM blood-based dosimetry practiced by IKN with the MTA calculated among different dosimetry approaches.
2. To determine the correlation between the BDpA calculated by EANM blood-based dosimetry practiced by IKN with the BDpA calculated among different dosimetry approaches.
3. To suggest credible dosimetry approaches for MTA estimation as the standard to be considered by IKN in future pre-therapeutic dosimetry for ^{131}I therapy in patients with DTC.

1.4 Study Hypothesis

1.4.1 Null Hypothesis

1. There is no significant difference between the MTA calculated by EANM blood-based dosimetry practiced by IKN with the MTA calculated among different dosimetry approaches. (Image-based/ RM-based/ Simplified Image-based)

2. There is no correlation between the BDpA calculated by EANM blood-based dosimetry practiced by IKN with the MTA calculated among different dosimetry approaches. (Image-based/ RM-based/ Simplified Image-based)

1.4.2 Alternative Hypothesis

1. There are significant differences between the MTA calculated by EANM blood-based dosimetry practiced by IKN with the MTA calculated among different dosimetry approaches. (Image-based/ RM-based/ Simplified Image-based)
2. There is correlation between the BDpA calculated by EANM blood-based dosimetry practiced by IKN with the MTA calculated among different dosimetry approaches. (Image-based/ RM-based/ Simplified Image-based)

1.5 Significance of the Study

Estimating the MTA yield through the calculation of BDpA from various dosimetry methods holds significance, given the absence of a universally accepted approach acknowledged by the IKN. The lack of a standard method has led to discrepancies in MTA estimations among different institutions, as they adopt diverse dosimetry techniques. (Hindorf et al., 2010; Pandit-Taskar et al., 2021; Schwartz et al., 2012). The significance of this study lies in its potential to suggest a standard approach for the pre-therapeutic dosimetry process in IKN, thereby reducing the variability in MTA estimations that can impact the treatment efficacy. By conducting a comparative analysis of BDPA and MTA estimated by EANM blood-based dosimetry approach practice by IKN and contrasting it with image-based and RM-based approaches, this research seeks to identify the most accurate and reliable dosimetry approach. This will facilitate and enhance treatment quality and outcomes for patients with DTC. Additionally, understanding the correlation and differences among the studied

approaches can provide more comprehensive framework for future dosimetry standard, ultimately contributing to more consistent and effective patient care. Thus, this study aims to offer valuable insights into dosimetry approach selection for pre-therapeutic dosimetry in ^{131}I therapy at IKN's Nuclear Medicine Department. However, the ultimate choice of dosimetry approach rests with IKN's preferences.

1.6 Conceptual Framework

The independent variable of this study was the type of dosimetry approaches used to calculate the dependent variables, which were the BDpA and the MTA. Figure 1.1 illustrated the conceptual framework of this study to determine the significant difference and correlation between the MTA estimated by the EANM blood-based dosimetry approach practiced by IKN with the MTA estimated by image-based dosimetry approach, RM-based approach, and simplified image-based approach.

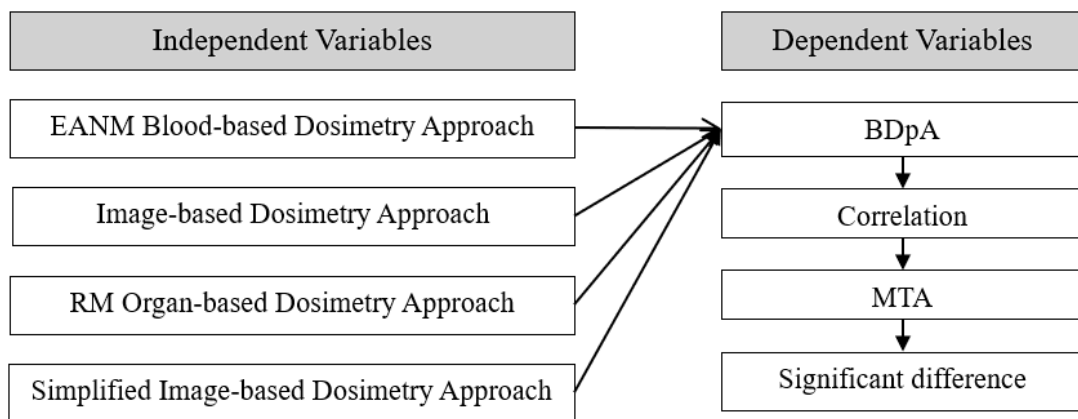


Figure 1.1 Conceptual framework.

CHAPTER 2

LITERATURE REVIEW

2.1 Radioiodine Therapy

Radioiodine (RAI) therapy refers to the systemic administration of ^{131}I -sodium iodide or ^{131}I -potassium iodide (^{131}I) to selectively irradiate thyroid remnants, microscopic differentiated thyroid cancer (DTC) or other non-resectable or partially resectable DTC (Luster et al., 2008). Due to ^{131}I unique metabolic properties, it is able to mimic the behaviour of iodine in thyroid hormone production, it is considered the ideal radionuclide for specifically irradiating thyroid cancer tissue since thyroid can naturally uptake the metabolized ^{131}I (Mazzaglia et al., 2019). Study conducted by demonstrated that using ^{131}I therapy for intermediate and high-risk DTC patient for remnant ablation and metastasis treatment improved their disease specific mortality (Dorn et al., 2003). As mentioned by Luster et al., 2008 there are primarily two therapeutic approaches for determining the amount of ^{131}I activity prescribed for DTC treatment, the empirical fixed activity approach for generalized ^{131}I therapy and the pre-therapeutic blood-based dosimetry assessment which customizes the maximum tolerated activity (MTA) of ^{131}I for personalized treatment. Hackshaw et al., 2007 reported that the recommended range of fixed ^{131}I activities for remnant ablation after thyroidectomy is between 1.1 GBq and 3.7 GBq (30 mCi to 100 mCi) in a single administration. While for inoperable iodine-avid distant metastases, higher ^{131}I activities of 3.7 GBq to 7.4 GBq (100 mCi to 200 mCi) or more per administration are suggested to improve treatment efficacy and success (Jentzen et al., 2015). Although empirical dosage is more convenient, it is not be suitable for all DTC patient as standard fixed activities are not universally safe (Mäenpää *et al.*, 2008). Additionally using empirical fixed activities can result in underdosage reducing the

therapeutic effect or overdosing causing undesirable adverse side effects (Tuttle et al., 2006).

2.1.1 The European Association of Nuclear Medicine Blood-based dosimetry practiced by IKN.

Blood-based dosimetry is originated by Benua and Leeper (1986) that aimed to estimate the D_{BL} or D_{RM} (Gy) per activity administered (GBq) which in turns used to define the personalized MTA of the ^{131}I therapy. (Mazzaglia et al., 2019). The EANM guidelines indicate that the administered ^{131}I activity should be limited to prevent myelotoxicity. To ensure safety, the prescribed activity should result in a dose D_{BL} , a proxy for radiation dose to the bone marrow D_{RM} , of less than 2 Gy to avoid bone marrow suppression or hematologic toxicity (Lassmann et al., 2008). This widely accepted dose limit was initially introduced by Benua et al., 1962 and continues to be a standard practice in clinical settings.

This study focuses on the EANM pre-therapeutic blood-based dosimetry assessment conducted by IKN, following a procedure similar to that outlined in a study by Mohamad Aminudin et al., 2017. The procedure commences with the precise measurement of the initial activity (A_0) of ^{124}I . This is achieved by placing the radionuclide on a sugar cube and enclosing it within a copper container to filter low-energy x-rays, with activity measurement performed using a dose calibrator. The ^{124}I diagnostic radiotracer is then orally administered in a volume of less than 30ml, with A_0 ranging from 30 MBq to 60 MBq. Radiotracer counts are obtained at approximately 1-2 hours, 24 hours, and ≥ 72 hours post-administration, as recommended by Jentzen et al., 2015. Sequential blood samples (approximately 1.5-2.5 ml) are collected and measured using a well counter. External whole-body counting is conducted at a

distance of 2 meters from the gamma probe detector, in both anterior and posterior views, to minimize sensitivity to redistribution, as advised by Lassmann et al., 2008.

Following the collection of counts from blood samples and whole-body measurements at three time points, the radionuclide matched-pair approach is then performed by projecting the measured ^{124}I -based uptake values (%) in both blood and whole-body compartment at each time point corresponding to ^{131}I uptake values (%) based on the physical half-life correction formalism as establish in the study of Jentzen et al., 2015 referring to the Equation (1). This projection is done based on the assumption that each iodine has identical radio pharmacokinetics.

$$U_{131}(t) = U_{124}(t) \cdot e^{\left(0.69 \frac{t}{T_{p124}}\right)} \cdot e^{\left(-0.69 \frac{t}{T_{p131}}\right)} \quad (1)$$

The obtained ^{131}I -based blood and whole-body uptake values (%) at three time points were inputted into the OLINDA/EXM software (Version 1.1), along with the respective time differences post administration of the ^{124}I radiotracer (h), to generate a time-activity curve. Using the bi-exponential curve-fitting feature of the software, the time-activity curves were fitted, and the corresponding retention functions were integrated from zero to the last data point collected at 96 hours by the software. This process allowed for the derivation of the τ_{BL} and τ_{WB} , both expressed in hours and denoted as the number of disintegrations in the software. According to the EANM guidelines, the bi-exponential fitting is adequate for determining both the τ_{BL} and τ_{WB} , which represent the integral of the time-activity curve describing the cumulative activity in the respective source organs (blood and whole body) as a function of time after the administration of the activity (Lassmann et al., 2008). The τ_{BL} obtained in hours needs to be normalized to per millilitre of blood, as indicated in Equation (5), to

yield the τ_{BL}^{1ml} required in the D_{BL} and D_{RM} dosimetry model formalisms for dose calculation.

The total blood volume (TBV) in ml for each patient is calculated based on method propose by Pearson et/all (1995) with different formalism customizes based on gender. As shown in Equation (2) is the TBV estimates for male patient while in Equation (3) is for female patient. Whereas Equation (4) shows the formula for surface area estimation.

$$TBV(Male) = [(1486 \times S) - 825] + (1578 \times S) \quad (2)$$

$$TBV(Female) = [(1.06 \times age) + (822 \times S) - 825] + (1395 \times S) \quad (3)$$

$$S_a = W^{0.425} \times H^{0.725} \times 0.007184 \quad (4)$$

Where age is expressed in years, S_a is the surface area expressed in m^2 , H is the patient's height expressed in cm, and W is the patient's mass expressed in kg.

$$\tau_{BL}^{1ml} = \frac{\tau_{BL}}{TBV} \quad (5)$$

Where τ_{BL}^{1ml} is the residence time in 1 ml of blood as shown in Equation (5) is expressed in hml^{-1} , blood residence time is expressed in h, and TBV is the total blood volume expressed in ml. The resulted τ_{BL}^{1ml} and τ_{WB} will be substituted into the EANM blood-based dosimetry model proposed by (Lassmann et al., 2008) to determine the D_{BL} to surrogate the D_{RM} in Equation (6). The D_{BL} obtained was then used to estimate the personalized MTA for each patient based on Equation (11).

$$D_{BL} = A_0 \left[108 \cdot \tau_{BL}^{1ml} + \frac{0.0188}{(m_{WB})^{\frac{2}{3}}} \cdot \tau_{WB} \right] \quad (6)$$

Where D_{BL} is the absorbed dose expressed in Gy, A_0 is the administered tracer activity expressed in GBq. m_{WB} is the patient's mass expressed in kg, τ_{WB} is the whole-body residence time expressed in h.

The first component in the EANM-blood based dosimetry model shown in Equation (6) was estimated by Benua & Leeper, 1986. This component, denoted as D_{BL} , accounts for the energy absorption of 187 keV emitted beta particles per radioactive decay in the blood, equating to 108 Gy·ml/(GBq·h). It solely considers self-irradiation of the blood by beta particles and is supported by Monte-Carlo simulations (Lassmann et al., 2008). Additionally, the second component, $\frac{0.0188}{(m_{WB})^{\frac{2}{3}}}$ (Gy/GBq), was derived from Monte-Carlo simulations and represents the gamma contribution to the mean D_{BL} per unit activity dispersed throughout the body (Stabin et al., 2005). The EANM blood-based dosimetry model closely resembles the Benua dosimetry model in estimating D_{BL} , with notable agreement. This model has been adopted by IKN since 2015 as a radiation safety precaution due to its higher D_{BL} -derived MTA estimation as recommended by EANM guidelines (Lassmann et al., 2008). Figure 2.1 illustrates the flowchart of the pre-therapeutic blood-based dosimetry assessment practiced by IKN.

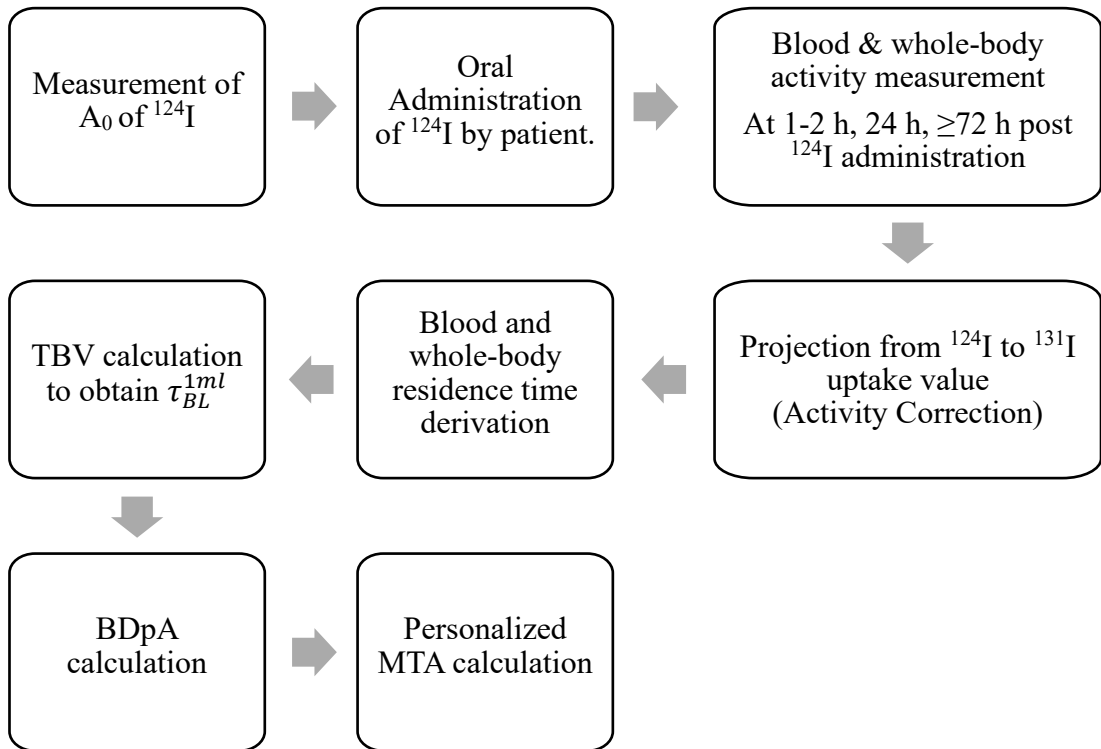


Figure 2.1 Flowchart of Pre-Therapeutic Blood Based Dosimetry Assessment Practiced By IKN.

2.1.2 Red Marrow as an Organ at Risk

Red marrow (RM), a vital tissue in the human body, plays a crucial role in the production of blood cells. Comprising hematopoietic cell parenchyma and a supportive stroma, RM stands out as one of the body's most radiation-sensitive tissues. (Caracappa et al., 2009). In the context of radioiodine therapy, RM is identified as an organ at risk (OAR), with hematopoietic RM being the primary OAR of concern (Songprakhon et al., 2020). When subjected to radiation therapy, the RM can experience a decrease in white blood cells, red blood cells, and platelets, which can be known as myelosuppression with the severity depending on the treated body part and radiation dosage. (Caracappa et al., 2009)

RM holds significance as the initial dose-limiting organ in systemic radionuclide therapies like radioimmuno- or radiopeptide therapy. Consequently,

accurate estimation of radiation absorbed doses to the RM becomes imperative to avert myelotoxicity. (Behr, et al., 2002). Various studies have investigated the absorbed dose in RM during radioiodine therapy. Findings indicate that keeping the absorbed dose to RM below 2 Gy is crucial to avoid haematological toxicity, solidifying the RM's role as the primary dose-limiting tissue in systemic radionuclide therapy. (MACEY et al., 1995)

Additionally, the use of the absorbed dose to the blood as a surrogate for RM is underscored as a practical approach to mitigate haematological toxicity in radioiodine therapy (Songprakhon et al., 2020). The exploration of personalized dosimetry is underway, aiming to enhance the precision of radiation dose estimation in radioiodine therapy (Pacilio et al., 2022). To ensure accuracy in estimating the percentage of RM exposed to radiation, the delineation of the patient's actual RM is crucial. This delineation is typically achieved through manual or semi-automatic contouring based on PET/CT images, followed by extracting the mean absorbed dose (Abu-Gheida et al., 2021).

2.1.3 The Rationale of Absorbed Dose of Blood, Red Marrow and Blood Dose per Activity

According to the EANM guidelines detailed by Lassmann et al., 2008 the effective dose from irradiation sources contributing to the absorbed dose in the body includes beta particles released from activity retained in blood and penetrating gamma rays emitted from activity distributed throughout the body. Consequently, when calculating the D_{BL} in pre-therapeutic blood-based dosimetry assessments, measurements of activity retention are necessary for only two compartments which is the blood itself and the entire body (Luster et al., 2008).

The Medical Internal Radiation Dose (MIRD) Committee of the Society of Nuclear Medicine developed the MIRD schema, which employs a specific mathematical framework, as detailed by Maxon (1999). This schema encompasses variables associated with the physical process of energy deposition resulting from irradiation and the biological systems involved in calculating absorbed doses. The absorbed dose formula is defined in Equation (7) below, where \tilde{A} is the cumulated activity, A_0 is the initial administered activity, S is the mean absorbed in the target organ per decay in the source organ and τ is the residence time (Ferrer et al., 2010).

$$D = \tilde{A} \times S$$

$$\frac{\tilde{D}}{A_0} = \frac{\tilde{A}}{A_0} \times S$$

$$\frac{\tilde{D}}{A_0} = \tau \times S \quad (7)$$

In the MIRD schema, the calculation of the D_{BL} and the D_{RM} involves summing the effects of both direct irradiation to the blood itself and indirect irradiation caused by gamma contributions stemming from activity dispersed throughout the body. The total absorbed dose to red marrow is the sum of the contribution of mean absorbed dose from relevant source organs. (Bolch et al., 2009; Hindorf et al., 2010). Specifically, the contribution of mean absorbed dose for red marrow is from red marrow $\tilde{D}_{RM \leftarrow RM}$ itself and the whole body $\tilde{D}_{RM \leftarrow WB}$. This summation process is expressed through specific equations within the MIRD framework as shown in Equation (8) and (9).

$$D_{RM} = \tilde{D}_{RM \leftarrow RM} + \tilde{D}_{RM \leftarrow WB}$$

$$\frac{\tilde{D}_{RM}}{A_0} = \tau_{RM} \times S_{RM} + \tau_{WB} \times S_{WB} \quad (8)$$

$$D_{BL} = \widetilde{A}_{BL} \times S_{BL} + \widetilde{A}_{ROB} \times S_{ROB} \quad (9)$$

In contrast to the broader terms of D_{RM} and D_{BL} , which encompass the radiation dose to the entire red marrow and blood, respectively, Blood dose per activity (BDpA) emerges as a more specific metric in the context of pre-therapeutic dosimetry and radiation oncology. BDpA provides a targeted and precise measurement of the radiation dose to the blood as shown in Equation (10). This specificity allows for a more accurate assessment of the potential health impacts of radiation exposure on the blood, particularly important in understanding the risks and effects of radiation therapy (Jentzen et al., 2015).

$$BDpA = \frac{\widetilde{D}}{A_0} \quad (10)$$

The personalized MTA is referred to as the largest and most effective ^{131}I dose that is considered safe to be prescribed to result in desired therapeutic outcome while preventing serious myelotoxicity by ensuring the prescribed activity resulted in the D_{BL} or D_{RM} that is below than 2 Gy (Luster et al., 2008; Miranti et al., 2015; Willegaignon et al., 2012). The MTA formalism that resulted in allowable maximum 2 Gy of dose delivered to the RM is expressed in Equation (11) which is originated by (Benua et al., 1962) and it is still clinically applicable until now.

$$MTA[GBq] = \frac{2 \text{ Gy}}{\widetilde{D}/A_0 [Gy/GBq]} \quad (11)$$

2.2 Multiple Dosimetry Approaches

2.2.1 Image-based dosimetry

Image-based dosimetry, an important aspect of radionuclide therapy, harnesses advanced molecular imaging like PET/CT to assess how radiopharmaceuticals

disperse within the body. This technique calculates the absorbed doses within tumours and adjacent healthy tissues, tailoring treatment strategies for individual patients (Michael Ljungberg and Gleisner, 2016). Specifically, in the realm of DTC, ^{124}I PET/CT imaging has emerged as a cornerstone for personalized therapy planning involving ^{131}I treatment. This methodology enables precise dosimetry calculations by gauging time-activity data, facilitating the determination of lesion dose-rate values crucial for optimizing therapeutic responses and reducing risks of healthy tissue toxicity. (Kuker et al., 2017; Plyku et al., 2022)

Moreover, these imaging-driven dosimetry approaches extend beyond thyroid cancer treatment. They play a pivotal role in Monte Carlo-based 3D dosimetry, offering comprehensive estimations of absorbed doses which is vital in radioiodine therapy (M. Ljungberg and Sjogreen Gleisner, 2018). Despite challenges like interpatient variability in absorbed doses and calibration intricacies, image-based technique presents an evolving landscape of safer and more effective treatment approaches (Michael Ljungberg and Gleisner, 2016). The integration of image-based dosimetry techniques in radionuclide therapy underscores a transformative shift toward personalized treatment regimens (Phan et al., 2008). Imaging dosimetry method account the trabecular bone volume of L2-L4 Lumbar spine and by assuming the RM mass in the lumbar vertebrae is proportional to trabecular bone volume, contributing 6.7% of the total RM mass (Shen et al., 2002). Beyond thyroid cancer, these methods hold promise for other malignancies, enabling fine-tuning of radiation doses while minimizing risks to healthy tissues (Ferrando et al., 2015).

Quantitative imaging accounts the variations in individual marrow mass, the calculation involved estimating RM mass from the lumbar vertebrae (L2-L4) trabecular bone volumes by scaling it with the Reference Man's trabecular bone

volume. Which is described in Equation (12) below. Where $V_{trab\ L2-L4}^{refman}$ is volume of the trabecular bone in lumbar vertebra (L2-L4) of refman (phantom) on a CT scan which is equal to 67cm^3 and $V_{trab\ L2-L4}^{patient}$ patient trabecular bone volume, $m_{L2-L4}^{patient}$ is the patient bone marrow mass while m_{L2-L4}^{refman} is reference man bone marrow mass. This approach assumes that RM mass is proportional to trabecular bone volume (Ferrer et al., 2010).

$$m_{L2-L4}^{patient} = m_{L2-L4}^{refman} \cdot \frac{V_{trab\ L2-L4}^{patient}}{V_{trab\ L2-L4}^{refman}} \quad (12)$$

To determine the D_{RM} from the lumbar trabecular volumes Equation (13) is used to correct the actual patient red marrow mass, estimated from the volume of the lumbar trabecular volume (Ferrer et al., 2010).

$$\frac{D_{RM \leftarrow RM}}{A_0} = \frac{\tau}{0.067} \times S_{RM} \times \frac{V_{trab\ L2-L4}^{patient}}{V_{trab\ L2-L4}^{refman}} \quad (13)$$

2.2.1.1 PET/CT image quantification

Image-based dosimetry in the context of PET/CT quantification is a method employed to compute the radiation dose delivered to a specific organ or tissue during radiotherapy. This approach utilizes PET/CT images to ascertain the distribution of the radioactive tracer within the body, enabling the calculation of the absorbed dose in the targeted tissue (Ferrando et al., 2015). Opting for PET/CT images in dosimetry presents several advantages compared to conventional methods. Notably, it allows for the consideration of patient-specific factors such as organ size, shape, and function. This level of personalization enhances the precision of treatment planning, ultimately leading to improved treatment outcomes and a decreased risk of adverse effects. (Zaidi

& Karakatsanis, 2017). However, a significant challenge in image-based dosimetry lies in the accurate quantification of PET/CT images. As previously mentioned, the precision of PET quantification is susceptible to various factors, encompassing the type of tracer utilized, the timing of the scan, and the physiological condition of the patient. (Brosch-Lenz et al., 2023).

2.2.2 Simplified Image-based dosimetry

Simplified Excel spreadsheet for image-based dosimetry was proposed by Songprakhon et al., 2020 to perform radioiodine RM dosimetry and compare its results with commercial software. The author highlighted the laborious and invasive nature of blood dosimetry and the high-cost limitations associated with commercial image-based dosimetry software. Hence the author emphasizes the need for practical and cost-effective methods to calculate absorbed doses to the red marrow, considering the safety and efficacy of the treatment. All the data was exported into a prepared Excel spread sheet. The spread sheet required the exact administration time and activity of ^{124}I , patient's demographic data (height, weight and gender) and whole-body total integral activity for all 3 time points, 1hr, 24 hr, and ≥ 72 hr post injection to perform estimation.

The Excel sheet consider contains several aspects, which include the consideration of the background correction count, where the background activity will be subtracted from the average activity of the whole body. The net whole-body activity will be the product of the number of pixels in the WB image and the subtracted average WB activity.

The researcher utilizes equipment efficiency to determine activity, similar to OLINDA/EXM image-based software. It involves computing the whole-body activity

for each time point as a fraction of the administered activity (FAA) using a mono-exponential function within MS Excel. It signifies the fraction of administered activity at time 't,' with 'A' and 'λ' being constants obtained through fitting. The τ_{WB} will be obtained by calculating the integral using Equation (14).

$$FAA(t) = A(t) \times e^{-\lambda \times t}$$

$$\tau_{WB} \int_0^{\infty} FAA(t) dt \quad (14)$$

The author then uses estimation of blood and RM technique proposed by Thomas et al., 1993, where the blood residence time τ_{BL} can be estimated by using 14% from τ_{WB} referring to Equation (15). Followed by $D_{RM \leftarrow ECF}$ can be estimated by using activity concentration in blood and the red marrow extracellular fluid fraction (RMECF) of 0.19 based on Equation (16).

$$\tau_{BL} = 0.14 \times \tau_{WB} \quad (15)$$

$$D_{RM \leftarrow ECF} = A_0 \times 0.19 \times m_{RM,phantom} \times S_{RM \leftarrow RM,phantom} \quad (16)$$

In this scenario, there were only two specific source organs considered which is the RM and the remaining of body (RoB). The calculation of the residence time of the remainder of the body (τ_{RoB}) as shown in Equation (17) involves subtracting the of specific τ_{BL} from τ_{WB} . The S value used for the RoB to RM was obtained from the anthropomorphic phantoms ($S_{RM \leftarrow RoB,phantom}$). However, for patient-specific calculations, the S value for the remainder of the body to red marrow ($S_{RM \leftarrow RoB,patient}$) was determined using a linear scaling method as shown in Equation (18). Finally, the D_{RM} can be determined by the Equation (19), while MTA can be determined by Equation (11).

$$D_{RM \leftarrow RoB} = A_0 \times (\tau_{WB} - \tau_{BL}) \times S_{RM \leftarrow RoB, phantom} \quad (17)$$

$$S_{RM \leftarrow RoB, patient}$$

$$= \left[S_{RM \leftarrow RoB, patient} \times \frac{m_{WB, phantom}}{m_{WB, phantom} - m_{RM, phantom}} - S_{RM \leftarrow RoB, patient} \times \frac{m_{RM, phantom}}{m_{WB, phantom} - m_{RM, phantom}} \right] \times \frac{m_{WB, phantom}}{m_{WB, patient}} \quad (18)$$

$$D_{RM} = D_{RM \leftarrow ECF} + D_{RM \leftarrow RoB} \quad (19)$$

The article states that there is no statistical difference after comparing the results of the simplified Excel spreadsheet with those obtained from commercial image-based dosimetry software, highlighting the potential for this approach to offer a feasible alternative for routine clinical practice.

2.2.3 Red Marrow-based (OLINDA)

The RM-based dosimetry will be represented by using the OLINDA/EXM Software. This was designed to calculate internal doses for various radionuclides used in diagnostics and therapy. It replaced the MIRDOSE 3.1 code, offering improved capabilities and models, including the ability to customise organ masses for each patient leading to more personalized dose calculations (Jeffrey A. Siegel et al., 2005). Developed by Michael Stabin, PhD, in 2004, written in the Java (Sun Microsystems) programming language, it was based on Radiation Dose Assessment Resource (RADAR) Task Group of the Society of Nuclear Medicine methods. The software's outputs were considered trustworthy, given its capability to adjust organ masses to patient-specific values, leading to more personalized dose calculations, particularly for RM dose predictions. Additionally, the software's new section for exponential modelling now enables fitting data using one to three exponential functions. It includes regression kinetic analysis code for user-supplied patient biokinetic data.

The software was designed to be user-friendly, requiring users to specify only the radionuclide used, the types of phantom or organ models, and parameters related to the biokinetics of the radionuclide, such as residence times for dose computation (Jeffrey A. Siegel et al., 2005). The software offers a range of whole-body anthropomorphic phantom models, including adult male, adult female, children at various ages (1, 5, 10, 15 years old), newborn, and women at different trimesters. These predictions were validated against established literature and the MIRDOSE 3.1 code, earning recognition from the Food and Drug Administration (FDA) (Jeffrey A. Siegel et al., 2005).